ADVANCED FUNCTIONAL MATERIALS
www.afm-journal.de

A Low-Permeability and Flexible Polymer Tube for Long-Life Fiber Lithium-Ion Batteries

*Haibo Jiang, Xiaocheng Gong, Jiaqi Wang, Zhe Yang, Chuanfa Li, Yao Long, Chenhao Lu, Shiqi Sun, Kun Zhang, Yingfan Chang, Pengzhou Li, Xiangran Cheng, Huisheng Peng, and Bingjie Wang**

Fiber lithium-ion batteries (FLIBs) hold great promise for powering wearable electronics. However, their practical application is hindered by limited cycle and calendar life, primarily due to the loss of active Li caused by water vapor permeation through the encapsulation layer. To address this challenge, a low-permeability and high-flexibility tetrafluoroethylene hexafluoropropylene copolymer (FEP) tube is presented to continuously encapsulate FLIBs by melting extrusion method. Owing to the inherent hydrophobicity of fluorine resins and appropriate crystallinity of the polymer matrix, FEP tubes exhibited significantly low vapor permeability, with a water vapor transmittance rate (WVTR) of 0.3 mg·day^{-1}·pkg^{-1}, 15 times lower than that of the nylon 12 tubes (4.6 mg·day^{-1}·pkg^{-1}). Leveraging the low permeability and elastic modulus of FEP tubes, FLIBs demonstrate a capacity retention of 80.05% after 180 cycles and exceptional flexibility with a capacity retention of 98.32% after 10 000 bending cycles, showcasing superior performance compared to the conventional polymer tubes (for example, the capacity of PP-FLIBs declined by 20.68% after 30 cycles). This work presents a general and efficient strategy for continuously encapsulating FLIBs, effectively extending their cycle and calendar lifetime of FLIBs, thereby enhancing their practical viability for wearable electronic applications.

1. Introduction

Due to their unique 1D configuration, exceptional weavability, and energy storage performance, FLIBs are regarded as promising energy supply systems for various portable electronic devices.[1] Continuous advancements in fabrication techniques have enabled FLIBs to achieve scalable production,[2] thereby bolstering the prospects of commercializing wearable energy storage fabrics. Despite notable progress in improving the energy density and rate performance of FLIBs through designing the electrode structure[3] and optimizing active materials,[4] another vital yet seemingly overlooked aspect is their limited lifetime, which fails to meet the actual application requirements in ambient air. The lifetime and aging processes of scalable FLIBs mainly depend on the continuous packaging methods and packaging materials, which have not been systematically studied so far.

Obviously, packaging materials play a crucial role in extending the cycle and calendar life of FLIBs. Similar to commercial lithium-ion batteries,[5] the infiltration of water vapor from the atmosphere through the encapsulation layer results in electrolyte decomposition and active Li loss, ultimately diminishing the cycle and calendar life of FLIBs. While some studies have explored potential packaging methods for flexible planar electronic devices,[6] they were unsuitable for the continuous production of FLIBs due to the complex manufacturing process and high curvature of FLIBs. Therefore, there is an urgent need to develop an encapsulation layer with both low permeability and high flexibility through a continuous manufacturing process to prolong the lifetime and enhance the practical feasibility of FLIBs.

Herein, we have, for the first time, proposed and successfully validated that FEP tubes serve as the encapsulation layer to enhance storage and cycling performance of FLIBs through a continuous packaging process (Figure S1, Supporting Information). The FEP tubes demonstrated exceptional production scalability, enabling continuous production in lengths of tens of kilometers or longer, while maintaining high uniformity in weight (Figure S2, Supporting Information) and dimension (Figure S3, Supporting Information). Due to the inherent hydrophobicity of fluorine resins and densely packed polymer chains, FEP tubes displayed considerably low vapor permeability. The water vapor transmittance rate (WVTR) of FEP610 tube stabilized at 0.5 mg·day^{-1}·pkg^{-1}, much lower than the conventional polymer tubes (such as PP, PE, and PA12 tubes). Subsequently, depending on the copolymer composition, the FEP810 tube exhibited higher crystallinity (≈23.79%) among the FEP tubes, resulting in a lower

H. Jiang, X. Gong, J. Wang, Z. Yang, C. Li, Y. Long, C. Lu, S. Sun, K. Zhang, Y. Chang, P. Li, X. Cheng, H. Peng, B. Wang
State Key Laboratory of Molecular Engineering of Polymers
Department of Macromolecular Science, Institute of Fiber Materials and Devices, and Laboratory of Advanced Materials
Fudan University
Shanghai 200438, China
E-mail: wangbingjie@fudan.edu.cn

The ORCID identification number(s) for the author(s) of this article can be found under https://doi.org/10.1002/adfm.202408529

DOI: 10.1002/adfm.202408529

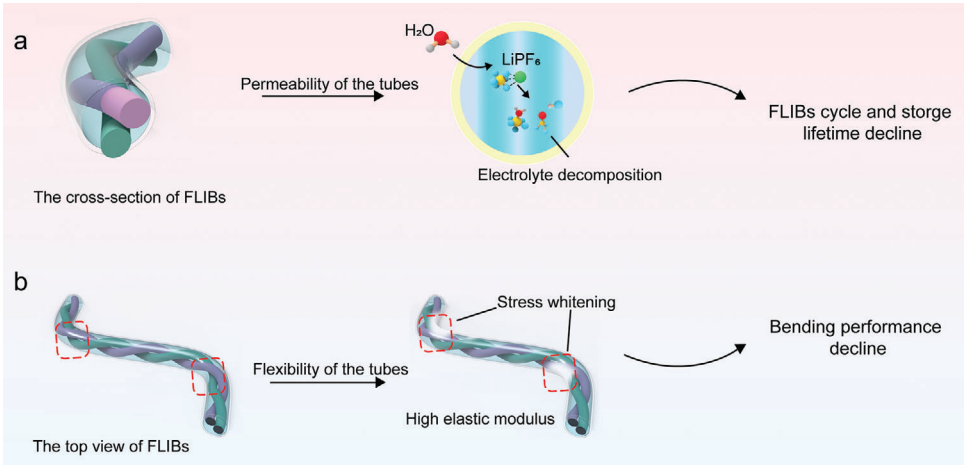

Figure 1. Impact of the encapsulation tubes on the calendar life, cycle life and bending performance of FLIBs. (a) Water vapor infiltration from the air through the encapsulation layer cause electrolyte decomposition and active Li loss, resulting in poor cycle and calendar life. (b) Encapsulation tubes with higher elastic modulus bear more stress under the same strain, leading to stress whitening or even fracture.

WVTR (0.3 mg·day^{-1}·pkg^{-1}). The resultant FEP810-FLIBs made optimal use of low permeability of the encapsulation tube, resulting in a capacity retention of 80.05% after 180 cycles for the FLIBs. More importantly, the inclusion of hexafluoropropylene copolymer segments allowed for free volume within the tubes, ensuring flexibility to meet the needs of bending and weaving. Consequently, with a lower elastic modulus (62.81 MPa), FEP810-FLIBs achieved better bending performance (10 000 bending cycles with 98.32% capacity retention). The successful extrusion and utilization of FEP810 tubes significantly improved the cycle and calendar life of FLIBs, further promoting practicality and commercialization prospects. It is noteworthy that the high transparency of FEP tubes, combined with their low permeability and high flexibility, render them valuable for the packaging of fiber sensors and fiber solar cells in the field of smart wearables.

2. Results and Discussion

The packaging methods and materials have a significant impact on the calendar life, cycle life, and bending performance of FLIBs. Typically, the continuously produced FLIBs consist of intertwined positive and negative fibers, which were subsequently encapsulated within a polymer tube (Figure S4, Supporting Information). However, the presence of free volume within the encapsulation tube allows water vapor molecules from the air to permeate into the battery, resulting in electrolyte decomposition and a decline in lifetime (**Figure 1a**). Additionally, encapsulation tubes with higher elastic modulus bear more stress under the same strain, leading to stress whitening or even fracture, which can damage the flexibility and weavability of FLIBs (Figure 1b). Modifying the packaging material emerges as one of the most direct and effective ways to improve the cycle and calendar life of FLIBs. An ideal packaging material should offer the dual advantages of low permeability and high flexibility to ensure improved flexibility and prolonged lifetime for the practical application of FLIBs in wearable electronic devices.

Water vapor permeability is a crucial factor in selecting packaging materials. To explore suitable materials for the continuous encapsulation of FLIBs, four typical polymer materials (PP, PE, PA12, and FEP), commonly employed in electronic packaging and various other industries,[7] have been chosen as packaging materials for the encapsulation of FLIBs. Among the nylon series, PA12 exhibited the lowest water absorption. PP and PE feature densely packed molecular chains, promoting high crystallinity[8] to prevent water molecule penetration. FEP, a copolymer of tetrafluoroethylene and hexafluoropropylene, combines exceptional stability, flexibility and hydrophobicity inherent in fluorine resins.[9] These materials theoretically possess low permeability and thus hold great potential as packaging materials for FLIBs. Subsequently, FLIBs encapsulated with transparent polymer tubes (Figure S5, Supporting Information) were manufactured continuously via melt extrusion using a single screw extruder (**Figure 2a**), without adding any additives.

Generally, the barrier property of polymer tubes is directly influenced by their molecular structure and functional groups. To confirm the variances in element and molecular structure among polymer tubes, comprehensive analysis was conducted on a representative set of four tubes. The EDS analysis (Figure S6, Supporting Information; Figure 2b) demonstrated a uniform distribution of elements, and confirmed that the characteristic elements of the four tubes corresponded to their respective molecular structures. Notably, the surface of FEP tube exhibited a strong fluorine signal response (Figure 2b), indicating an extremely strong repulsion of water molecules. Furthermore, the FTIR peaks of the other tube were found to be consistent with previous reports[10] (Figure S7, Supporting Information). Specifically, for the FEP tube, two strong characteristic peaks at 1130 and 1180 cm^{-1} were attributed to the stretching vibration peaks of the CF_2 and CF_3 functional groups, respectively (Figure 2c).

The water vapor transmission rate (WVTR) of polymers,[11] a direct parameter for evaluating their barrier properties against water molecules, can be conveniently measured. The WVTR (at 25 °C and 70% RH) of four tubes with identical inside and outside diameters (1 and 2 mm, respectively) showed significant differences (Figure 2d). A 50-cm-length PA12 tube exhibited a stabilized WVTR of 4.6 mg·day^{-1}·pkg^{-1}. Notably, the WVTR of

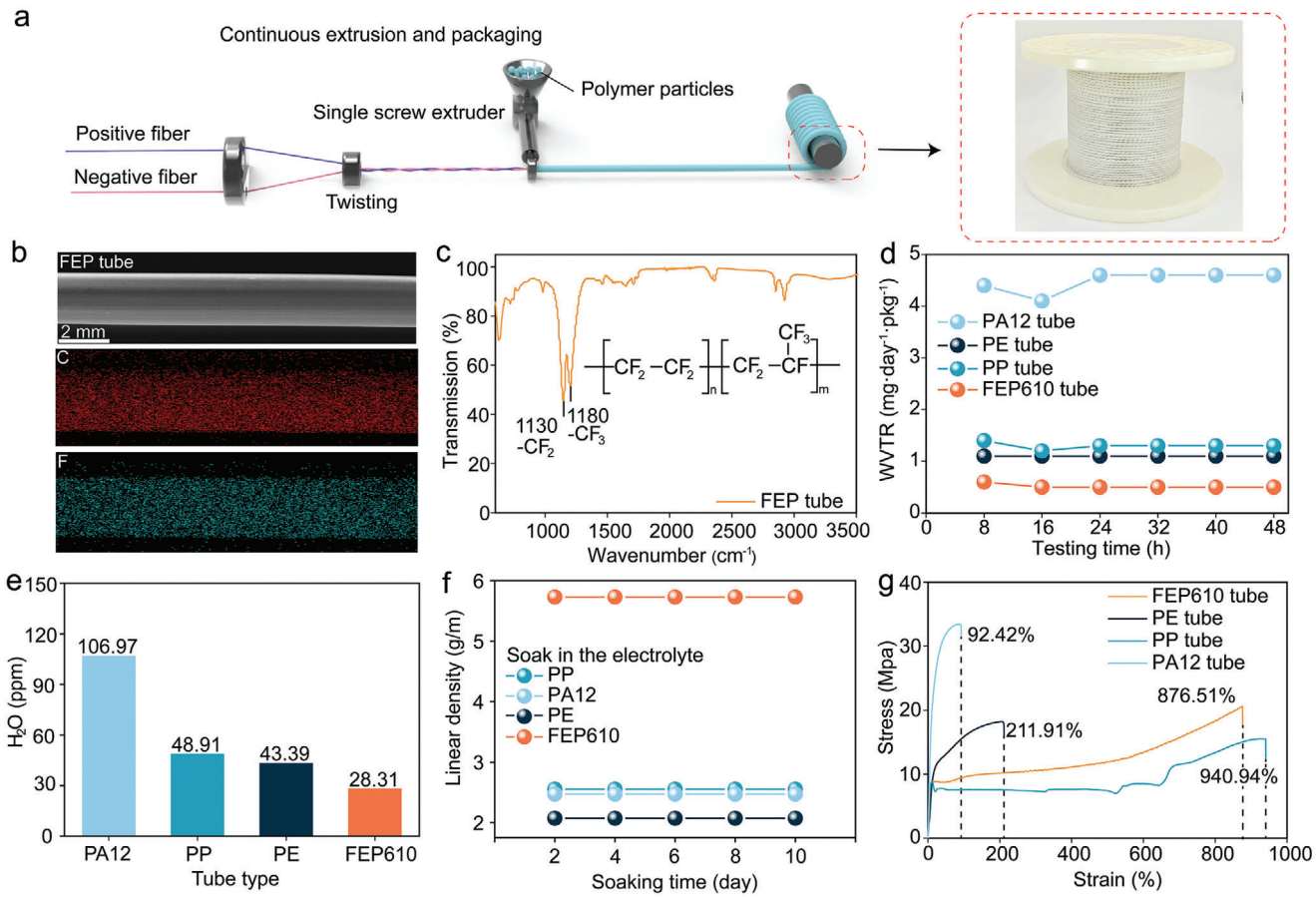

Figure 2. Continuous fabrication and characterization of the encapsulation tubes. (a) Continuous production of the encapsulation tubes allows for varying lengths to meet the needs of different FLIBs (b) EDS mapping demonstrates the distribution of carbon and fluorine signals on the tube surface. (c) FTIR spectra of the FEP tube in the range of 500–3500 cm^{-1}. (d) WVTR values of the four tubes at 25 °C and 70% RH. (e) Moisture content of the electrolyte encapsulated with the four tubes after 5 days in ambient air. (f) Linear density changes of the four tubes over soaking time. (g) Stress versus Strain curves of the four tubes.

FEP610 tube was the lowest, at only 0.5 $mg{\cdot}day^{-1}{\cdot}pkg^{-1}$ under the same test condition. In contrast, the WVTR of PE and PP tubes were 1.1 and 1.3 $mg{\cdot}day^{-1}{\cdot}pkg^{-1}$, respectively. It can be concluded that the differences in barrier properties of polymer tubes could be attributed to the different molecular structure (Figure S8, Supporting Information). Due to the hydrophobicity of fluorine resins and the tight arrangement of molecular chains, the FEP610 tube exhibited the best barrier performance among the four tubes. The low permeability of FEP610 was further confirmed by the moisture content of the electrolyte stored in ambient air for 5 days (Figure 2e). Subsequently, changing the test humidity still did not affect the WVTR trend of the four tubes (Figure S9, Supporting Information), confirming the superior barrier property of FEP610 tube to water vapor compared with the other tubes.

In order to verify the feasibility of the four tubes as packaging materials for FLIBs, 50-cm-length FLIBs were encapsulated with FEP610, PE, PP, and PA12 tubes, respectively. Following immersing in the electrolyte for 10 days, no changes in weight (Figure 2f) or color (Figure S10, Supporting Information) were observed, confirming that the electrolyte did not corrode or dissolve any of the polymer tubes. The resulting Coulombic Efficiency (Figure S11, Supporting Information) and internal resistance (Figure S12, Supporting Information) after formation procedure were within a reasonable range, indicating that the active materials could be activated normally. It should be noted that characteristic peaks in CV curves (Figure S13, Supporting Information) were essentially the same regardless of the change in packaging materials. These results indicated that all the packaging materials cannot react with the electrolyte, and the difference in the electrochemical performance of FLIBs was determined by the barrier properties of the encapsulation tubes.

To further demonstrate the influence of FEP610 tube on the lifetime of FLIBs, both calendar and cycle life tests were performed. The results of the cycle life test were depicted in **Figure 3a**. After 150 cycles, the capacity retentions of FLIBs encapsulated with FEP610, PE, PP and PA12 tubes were 75.28%, 43.40%, 33.11% and 1.04%, respectively, which was completely consistent with the trend of WVTR results above. Calendar life represents the aging of the battery during static storage,[12] characterized by noticeable capacity decline and internal resistance increase. Faster aging and shorter calendar life are extremely unfavorable to the commercialization process of batteries. Figure 3c shows that, after 5 days of storage, the internal resistances of

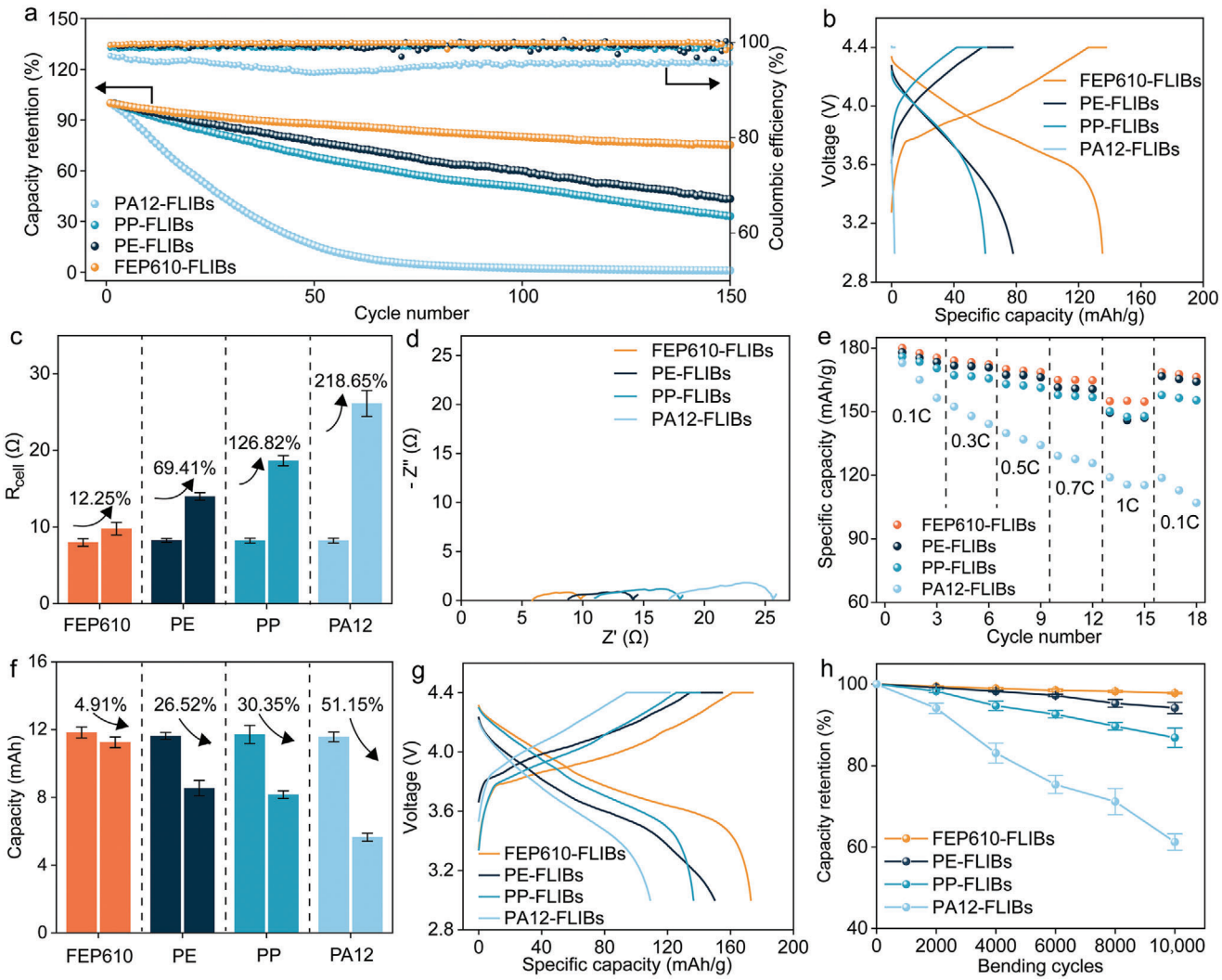

Figure 3. Electrochemical performance of FLIBs encapsulated with the four tubes. (a) Cycling performance of four FLIBs at 25 °C. (b) Corresponding charge–discharge profiles of (a) at the 150th cycle. (c) Internal resistance of FEP610-FLIBs, PE-FLIBs, PP-FLIBs, and PA12-FLIBs after 5 days of storage. (d) Typical Nyquist plots of four FLIBs after 5 days of storage. (e) Rate performance of four FLIBs. (f) Capacity decline of four FLIBs after 5 days of storage. (g) Charge–discharge curves of four FLIBs after 5 days of storage. (h) Capacity retention of four FLIBs under cyclic bending.

FLIBs increased by 12.25% (FEP610-FLIBs), 69.41% (PE-FLIBs), 126.82% (PP-FLIBs), and 218.65% (PA12-FLIBs), respectively. The Nyquist plots of FLIBs encapsulated with four tubes after storage can be observed in Figure 3d, with the FEP610 tube showing the lowest internal resistance. Capacity decline was represented in Figure 3f,g. After 5 days of storage, the capacity of PA12-FLIBs declined by 51.15%, while the capacity of FEP610-FLIBs only declined by 4.91%. The excellent barrier property of FEP610 tube improved the cycling and storage performance of FLIBs. Apart from the improvement of lifetime, the rate performance of FLIBs had also been enhanced, particularly for FEP610-FLIBs due to its superior barrier property. The rate test was conducted under various current rates and then returned to 0.1 C. The corresponding specific capacities of FEP610-FLIBs (Figure 3e) were 179.93 (0.1 C), 174.02 (0.3 C), 169.33 (0.5 C), 164.97 (0.7 C), and 155.10 (1 C) mAh g^{-1}, returning to 168.62 (0.1 C) mAh g^{-1}.

The flexibility and mechanical property of the encapsulation tubes were further characterized. The elastic modulus of the four tubes was measured by a universal material testing machine (Figure 2g). Elastic modulus is an index that reflects the ability to resist elastic deformation,[13] and a lower elastic modulus indicates that the tube has better ability to bend and deform. The elastic modulus of FEP610 tube was measured at 68.69 MPa, which was slightly lower than PE tube (80.52 MPa) and PP tube (87.41 MPa), significantly lower than that of PA12 tube (222.01 MPa). The presence of hexafluoropropylene segments within the molecular chain gives FEP a large free volume and considerable flexibility. Subsequently, the impact of different encapsulation tubes on the bending performance of the FLIBs was characterized through a bending test. FLIBs were bent around a point from 0 ° to 180 ° and back to 0 ° in a bending cycle, at a speed of 50 s^{-1} (Figure S14a, Supporting Information). After 10 000 cycles, the specific capacity of the four FLIBs was 175.82,

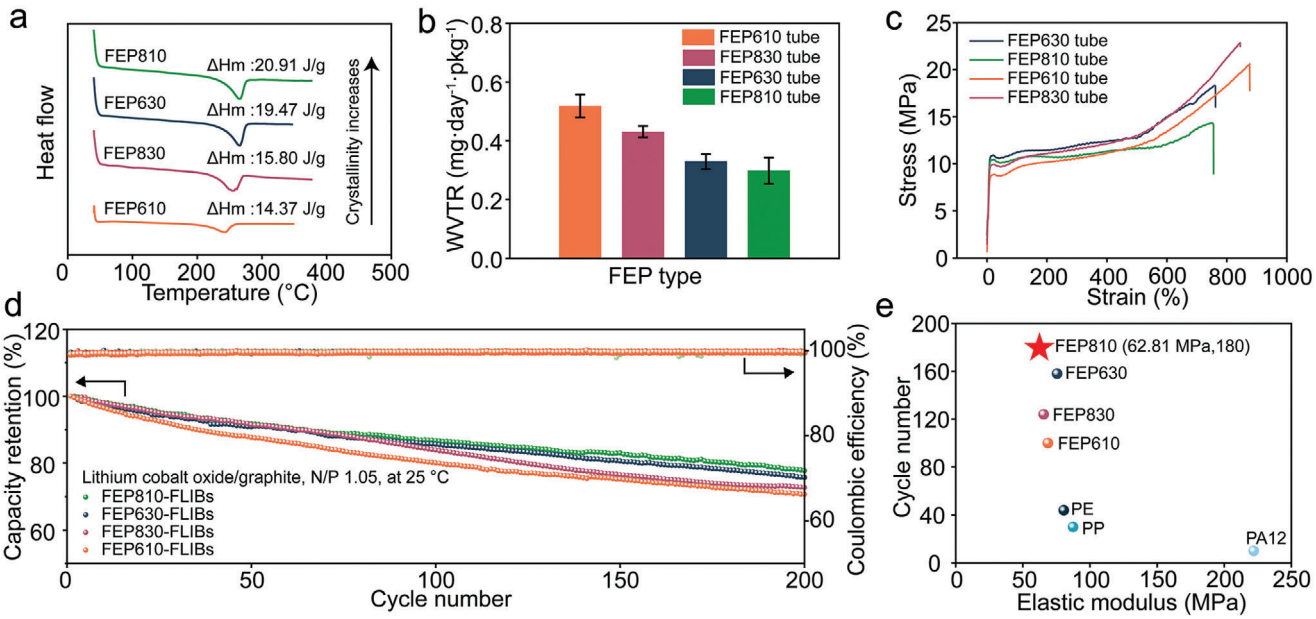

Figure 4. Characterization and electrochemical performance of four FEP-FLIBs. (a) DSC thermogram of FEP610, FEP630, FEP810, and FEP830 tubes. (b) WVTR values of the four FEP tubes at 25 °C and 70% RH. (c) Stress versus Strain curves of the four FEP tubes. (d) Cycling performance of four FEP-FLIBs at 25 °C. (e) Graph showing the elastic modulus of seven tubes versus cycle number of corresponding FLIBs. The capacity retention rate of FLIBs is 80%.

171.31, 159.28, and 113.91 mAh g^{-1}, respectively (Figure S14b, Supporting Information). Therefore, FEP610-FLIBs still had a capacity retention of 97.68%, while PA12-FLIBs only had a capacity retention of 63.28% (Figure 3h). These results clearly demonstrated that the excellent barrier property and flexibility of FEP610 tubes contributed to the longer lifetime and better bending property of FLIBs.

Overall, FEP610 tubes exhibited the best comprehensive properties among the four tubes. The influence of molecular chain compositions on the comprehensive performance of FEP was further investigated by employing different kinds of FEP resins. Depending on the copolymer composition, the crystallinity of FEP tubes can also vary greatly, ultimately leading to a difference in the moisture permeation.[14] In order to explore the effect of crystallinity on the barrier performance of the encapsulation tubes, four FEP tubes (FEP810, FEP630, FEP830, FEP610) with different compositions were obtained by melt extrusion. After calculation (**Figure** 4a), the crystallinity of FEP810 tube (≈23.79%) was significantly higher than the other three FEP tubes, while the FEP610 had the lowest crystallinity, ≈16.35%. As shown in Figure 4b, the FEP810 tube presented the lowest WVTR value among the FEP tubes, which gradually stabilized at 0.3 mg·day^{-1}·pkg^{-1} at 25 °C/70% RH, whereas the WVTR value of FEP610 tube was 0.5 mg·day^{-1}·pkg^{-1}. Obviously, with the increase in crystallinity, the permeability of water molecule gradually declined. Subsequently, electrochemical cycling tests were carried out to further confirm the permeability and practicability of FEP810 tube. FEP810-FLIBs exhibited superior cycling performance among four FEP-FLIBs. After 200 cycles (Figure 4d), the capacity retention of FEP810-FLIBs reached 77.77%, whereas the capacity retention of FEP610-FLIBs was only 70.67%. It is noteworthy that due to the presence of hexafluoropropylene in the main molecular chain, the crystallinity of FEP is generally at a low level, the appropriate increase of crystallinity will not have a great impact on the flexibility of FEP tube. According to the stress-strain curve (Figure 4c), the elastic modulus of FEP810 was the lowest among the four FEP tubes, at only 62.81 MPa. After the bending test (Figure S14c, Supporting Information), there was no change in the specific capacity of the four FEP-FLIBs. In particular, the capacity retention of FEP810-FLIBs remained at 98.32% after 10 000 bending cycles. Considering the permeability and flexibility of the tubes (Figure 4e), the FEP810 tube was the most suitable for continuously encapsulating FLIBs.

Finally, FEP810 tubes demonstrated strong stability, showing no change in WVTR after heating, bending, abrasing, UV aging tests, and impact tests (Figure S15, Supporting Information). The high stability, low elastic modulus, and low permeability of the FEP810 tube provided FLIBs with better flexibility and weavability. With the continuous preparation method, FEP810-FLIBs of various lengths (**Figure** 5a) can be produced according to actual requirements. It is remarkable that FEP810-FLIBs of different lengths showed excellent cycling performance (Figure S16, Supporting Information), with over 80% capacity retention after 150 cycles. As shown, a 20-cm-length FEP810-FLIB can be directly used to power electronic devices (Figure 5b). We further measured the capacity and internal resistance at various temperatures during storage (Figure S17, Supporting Information). As a result, FEP810-FLIBs can be easily woven into flexible (Figure 5c,d) textiles or sewn into handmade bags (Figure S18, Supporting Information) to power the phone more conveniently using an industrial rapier loom. Furthermore, the FEP810-FLIB textiles can also light up a variety of light-emitting fibers (Figure S19, Supporting Information) and light-emitting artworks (Figure 5e). In

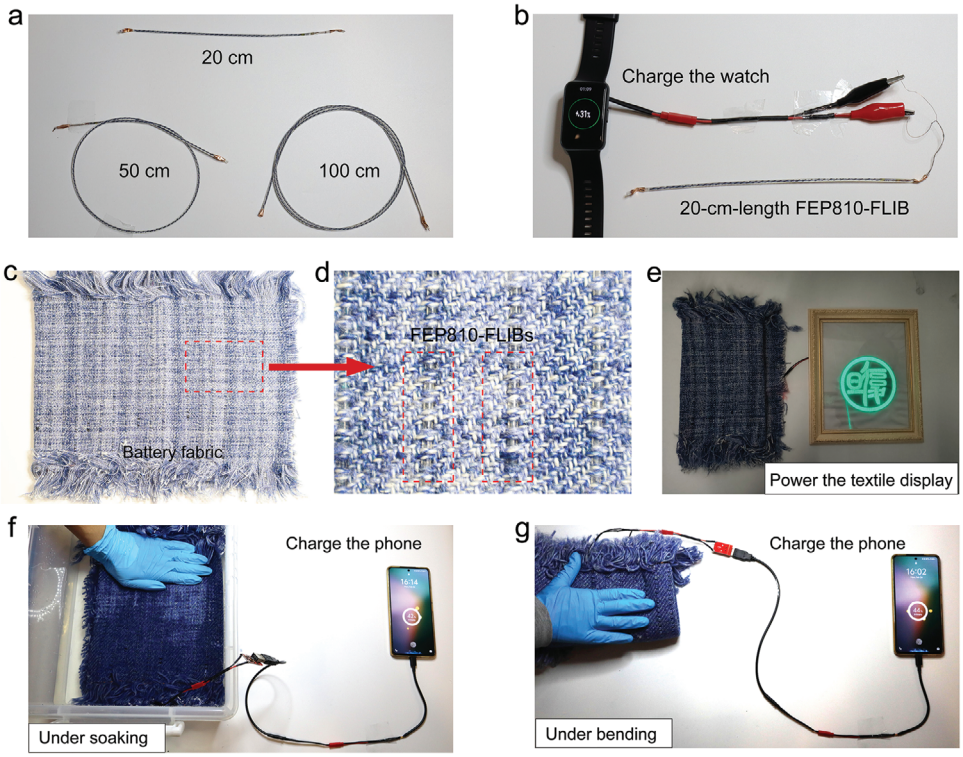

Figure 5. Applications of FEP810-FLIBs. (a) FEP810-FLIBs with various lengths. (b) A 20-cm-length FEP810-FLIBs can charge the watch. (c) FEP810-FLIBs can be easily woven into battery textile. (d) Partial view of (c). (e) The battery textile effectively powers the textile display. (f,g) The battery textile reliably charges the phone stably under conditions of bending and soaking in water, respectively.

addition to the excellent energy storage capability, FEP810-FLIBs textiles were also resistant to washing and mechanical abrasion. The FEP810-FLIBs textiles showed stable charging–discharging specific capacities after washing with detergent (Figure S20a, Supporting Information) and abrasing (Figure S20d, Supporting Information) for 10 000 cycles. Compared with traditional plate batteries, FEP810-FLIBs textiles had the advantages of flexibility, launderability and wearability, allowing them to power electronic devices under conditions of soaking (Figure 5f) and bending (Figure 5g).

3. Conclusion

In summary, a low-permeability and high-flexibility FEP810 tube has been prepared to encapsulate FLIBs continuously through melting extrusion. The inherent hydrophobicity of fluorine resins and densely packed polymer chains contribute together to the low water vapor permeability of the FEP810 tube, resulting in a capacity retention of FLIBs encapsulated with the FEP810 tube remaining at 80.05% after 180 cycles. Additionally, owing to the presence of free volume and low crystallinity (≈23.79%), the FEP810 tube exhibited a low elastic modulus and desirable high flexibility, resulting in a capacity retention of 98.32% after 10 000 bending cycles. The utilization of the FEP810 tube and continuous packaging offers a practical pathway to enhance the lifetime, flexibility, and practicality for FLIBs. We believe that with further optimization of the encapsulation tube, the commercialization process of FLIBs will be accelerated and the application scenario of energy storage fabric will become more extensive.

4. Experimental Section

Materials: Aluminum wire (99.99%, diameter 200 µm) and copper wire (99.99%, diameter 200 µm) were purchased from Nordisk Investment Co., LTD. N-methyl-2-pyrrolidone (NMP, analytical grade, ≥99.9%) analytical reagent was obtained from Sinopharm Chemical Reagent Co., LTD. Polyvinylidene fluoride binder (HSV 900, ≥99.5%), sodium carboxymethyl cellulose (CMC 2200, ≥99%), styrene butadiene Rubber (SBR TRD-104A, solid content 45.5% ± 0.1%) and lithium cobalt oxide (MA-EN-CA-0Q) were obtained from Shenzhen Kelude Company. Super-P (SP) conductive agent was obtained from Shanghai Huiping Chemical Co., LTD. Graphite (FSN-1) and separator (Celgard 2325) were purchased from Shanghai Shanshan Technology Co., LTD. FEP resin particles (FEP810, FEP830, FEP610, FEP630) were purchased from Zhejiang Juhua Co., LTD. PE (23 050) and PP resin particles (EP548R) were purchased from Wanhua Chemical Group Co., LTD. PA12 resin particle (PA3426) was obtained from Dupont. All materials were used as received without any further purification.

Preparation of Fiber Lithium-Ion Battery: The commercial aluminum wire and copper wire underwent cleaning in the ultrasonic cleaning zone, deionized water cleaning zone and drying zone, respectively. Graphite, SP, CMC, and SBR were mixed in the weight ratio of 92:3:1.4:3.6 for negative slurry preparation, with deionized water as the solvent. The solid content for graphite slurry was 51%. LCO, PVDF and SP were mixed in the weight ratio of 92:3:5 for positive slurry preparation, with NMP as the solvent. The solid content for the positive slurry was 55%. As illustrated schematically in Figure S1a (Supporting Information), aluminum wire and copper wire were coated with positive and negative slurries using a

starching machine, respectively. The loading weights of LCO and graphite were 170–190 mg m^{-1} and 95–105 mg m^{-1}, respectively. The capacity ratio of negative to positive electrode was ≈1.05, based on the actual specific capacity of 180 mAh g^{-1} for LCO and 340 mAh g^{-1} for graphite. As depicted schematically in Figure S1b (Supporting Information), the negative fibers were wrapped in 3-mm-width separator strips using a wrapping machine. Seven kinds of tubes were extruded using a single screw extruder. Among them, the extrusion melting temperature of FEP was 280–330 °C, while the melting extrusion temperatures of PP, PA12, and PE ranged between 190 °C and 250 °C. They were all cooled in 16 °C water. The traction speed was 4 m min^{-1}. As illustrated schematically in Figure S1c (Supporting Information), the positive and negative fibers were twisted using a home-made winch machine, and then the electrolyte was injected into the tube with a syringe. The two ends were sealed using an electric soldering iron.

Characterization of Tubes: Differential scanning calorimeter (TA, DSC 250) was employed to characterize the thermal performance of the tubes and calculate crystallinity. Four FEP tubes were measured over a temperature range of 40 to 350 °C at 20 °C min^{-1} with a sample weight of ≈10 mg in a high purity flowing nitrogen atmosphere (50 mL min^{-1}). Field emission scanning electron microscopy (Zeiss Gemini SEM500, FESEM) and Energy Dispersive X-ray Spectroscopy (EDS) was employed to investigate the surface morphology and element composition at 15 kV accelerating voltage. The surfaces of the polymer tube samples were coated with a 10 nm thick gold layer for SEM observations. Fourier transform infrared spectrometer (ThermoFisher Nicolet 6700) was utilized to analyze the characteristic functional groups of the tubes in the range of 500–3500 cm^{-1}. Their resolution and number of scans were equal to 4 cm^{-1} and 64, respectively. The elastic modulus of tubes was obtained using a universal material tester (Hengyi T0086) with a speed of 50 mm min^{-1} (Initial length is 20 mm). The 50-cm-length tubes with an inner diameter of 1 mm and an outer diameter of 2 mm were utilized to measure the water vapor transmission rate (WVTR) at 25 °C. The test humidities were set at 40%, 70%, and 100%, respectively. UV aging test (international standards of ASTM D4329-2005) was used to verify the stability and integrity of FEP810 tube after ultraviolet irradiation. First, FEP810 tubes were exposed to light intensity of 1.1 W m^{-2} at 70 °C for 8 h, and then experienced condensation at 50 °C for 4 h. A flexible testing device was used to simulate and test the impact performance of the tubes. One side of the tube was fixed, and a moving target impacted the tube at a speed of 7 cm s^{-1}, with a force length of 6 cm.

Electrochemical Measurements: For cycle life testing, FLIBs were galvanostatically charged at a rate of 0.3 C from 3 to 4.4 V and then charged at 4.4 V until the current dropped below 0.05 C rate. Subsequently, the FLIBs were discharged to 3 V at a rate of 0.5 C. Electrochemical impedance spectra (EIS) was conducted over a frequency ranging from 100 kHz to 0.1 Hz using an electrochemical workstation (CHI660E). Cyclic voltammetry (CV) curve was obtained with a scanning rate of 0.3 mV s^{-1} and a potential range from 3 to 4.4 V. To evaluate the rate performance, FLIBs were discharged at increasing current (0.1 C, 0.3 C, 0.5 C, 0.7 C, and 1 C) and charged at a constant 0.5 C within a voltage window of 3–4.4 V. For calendar life testing, FLIBs were stored at different temperatures for a specified time in an oven. Upon returning to room temperature, their capacity and internal resistance were measured.

Fabrication and Performance Tests of FLIBs Textiles: FEP810-FLIBs of various lengths can be sewn into the fabric using an industrial rapier loom. The size and capacity of the FLIBs textiles could be customized by adjusting the length and number of FLIBs. For instance, the FLIBs textiles (Figure 5c) comprised ten 100-cm-length FEP810-FLIBs to power both the phone and the textile display. Alternatively, fifteen 50-cm-length FEP810-FLIBs can be sewn into the interior of a handmade bag (Figure S18, Supporting Information) to serve as a power source. The washing tests for the FEP810-FLIBs textiles were conducted in accordance with the national standard GB/T 8629-2017. The FEP810-FLIBs textiles were washed at a speed of 90 r min^{-1}. The abrasion resistance tests for the FEP810-FLIBs textiles followed the national standard GB/T 3920-2008, with a pressure of 9 N and a friction distance of 10 cm.

Supporting Information

Supporting Information is available from the Wiley Online Library or from the author.

Acknowledgements

H.J. and X.G. contributed equally to this work. This work was supported by MOST (2022YFA1203001, 2022YFA1203002), NSFC (52222310, 22205039), and China Postdoctoral Science Foundation (2022M710733).

Conflict of Interest

The authors declare no conflict of interest.

Data Availability Statement

The data that support the findings of this study are available from the corresponding author upon reasonable request.

Keywords

encapsulation tube, fiber lithium-ion batteries, melt extrusion

Received: May 17, 2024
Revised: June 13, 2024
Published online: July 1, 2024

[1] a) J. Lee, B. Llerena Zambrano, J. Woo, K. Yoon, T. Lee, *Adv. Mater.* **2020**, *32*, 1902532; b) F. Mo, G. Liang, Z. Huang, H. Li, D. Wang, C. Zhi, *Adv. Mater.* **2020**, *32*, 1902151; c) T. Ye, J. Wang, Y. Jiao, L. Li, E. He, L. Wang, Y. Li, Y. Yun, D. Li, J. Lu, H. Chen, Q. Li, F. Li, R. Gao, H. Peng, Y. Zhang, *Adv. Mater.* **2022**, *34*, 2105120.

[2] J. He, C. Lu, H. Jiang, F. Han, X. Shi, J. Wu, L. Wang, T. Chen, J. Wang, Y. Zhang, H. Yang, G. Zhang, X. Sun, B. Wang, P. Chen, Y. Wang, Y. Xia, H. Peng, *Nature* **2021**, *597*, 57.

[3] a) X. Huang, C. Wang, C. Li, M. Liao, J. Li, H. Jiang, Y. Long, X. Cheng, K. Zhang, P. Li, B. Wang, H. Peng, *Angew. Chem., Int. Ed. Engl.* **2023**, *62*, 202303616; b) M. Liao, C. Wang, Y. Hong, Y. Zhang, X. Cheng, H. Sun, X. Huang, L. Ye, J. Wu, X. Shi, X. Kang, X. Zhou, J. Wang, P. Li, X. Sun, P. Chen, B. Wang, Y. Wang, Y. Xia, Y. Cheng, H. Peng, *Nat. Nanotechnol.* **2022**, *17*, 372; c) H. Jiang, M. Liao, Y. Chang, K. Zhang, Y. Jiang, B. Wang, H. Peng, *Acta Polym. Sin.* **2023**, *54*, 892.

[4] a) L. Chen, J. Zhou, Y. Wang, Y. Xiong, J. Zhang, G. Qi, J. Cheng, B. Wang, *Adv. Energy Mater.* **2023**, *13*, 2202933; b) Y. Gao, H. Hu, J. Chang, Q. Huang, Q. Zhuang, P. Li, Z. Zheng, *Adv. Energy Mater.* **2021**, *11*, 2101809; c) Y. Zhang, Y. Zhao, J. Ren, W. Weng, H. Peng, *Adv. Mater.* **2016**, *28*, 4524; d) Y. Zhang, K. Zeng, Y. Yang, W. Tang, H. Peng, *Acta Polym. Sin.* **2023**, *54*, 413.

[5] a) M. Kosfeld, B. Westphal, A. Kwade, *J. Energy Storage* **2022**, *51*, 104398; b) A. V. Plakhotnyk, L. Ernst, R. Schmutzler, *J. Fluorine Chem.* **2005**, *126*, 27; c) E. W. C. Spotte-Smith, T. B. Petrocelli, H. D. Patel, S. M. Blau, K. A. Persson, *ACS Energy Lett.* **2022**, *8*, 347.

[6] a) P. Y. Chen, M. Zhang, M. Liu, I. Y. Wong, R. H. Hurt, *ACS Nano* **2018**, *12*, 234; b) P. L. Floch, S. Meixuanzi, J. Tang, J. Liu, Z. Suo, *ACS Appl. Mater. Interfaces* **2018**, *10*, 27333.

[7] a) H. P. Araújo, J. S. Félix, J. E. Manzoli, M. Padula, M. Monteiro, *Radiat. Phys. Chem.* **2008**, *77*, 913; b) D. Carullo, A. Casson, C. Rovera,

M. Ghaani, T. Bellesia, R. Guidetti, S. Farris, *Food Packag. Shelf Life* **2023**, *39*, 101143; c) C. Cejudo Bastante, L. Casas Cardoso, M. T. Fernández Ponce, C. Mantell Serrano, E. J. Martínez de la Ossa-Fernández, *J. Supercrit. Fluids* **2018**, *140*, 196.

[8] a) M.-J. Khalaj, H. Ahmadi, R. Lesankhosh, G. Khalaj, *Trends Food Sci. Technol.* **2016**, *51*, 41; b) F. Seidi, E. Movahedifar, G. Naderi, V. Akbari, F. Ducos, R. Shamsi, H. Vahabi, M. R. Saeb, *Polymers* **2020**, *12*, 1701.

[9] a) M. E. Makowiec, G. L. Gionta, S. Bhargava, R. Ozisik, T. A. Blanchet, *Wear* **2022**, *502–503*, 204376; b) K. Ozeki, I. Nagashima, Y. Ohgoe, K. K. Hirakuri, H. Mukaibayashi, T. Masuzawa, *Appl. Surf. Sci.* **2009**, *255*, 7286; c) K. Yang, Q. Peng, M. Venkataraman, J. Novotna, J. Karpiskova, J. Mullerova, J. Wiener, M. Vikova, G. Zhu, J. Yao, J. Militky, *Prog. Org. Coat.* **2022**, *165*, 106775.

[10] a) S. N. Dimassi, J. N. Hahladakis, M. N. Daly Yahia, M. I. Ahmad, S. Sayadi, M. A. Al-Ghouti, *J. Hazard. Mater.* **2023**, *447*, 130796; b) C. Fan, Y.-Z. Huang, J.-N. Lin, J. Li, *Environ. Technol. Innovation* **2021**, *23*, 101798; c) P. Klingenberg, R. Brull, T. Fell, B. Barton, M. Soll, T. Emans, F. Bakker, G. Geertz, *Waste Manage.* **2024**, *178*, 135; d) A. Touris, A. Turcios, E. Mintz, S. R. Pulugurtha, P. Thor, M. Jolly, U. Jalgaonkar, *Results Mater.* **2020**, *8*, 100149; e) L. Wen, J. Zhang, T. Zhou, A. Zhang, *Vib. Spectrosc.* **2016**, *86*, 160; f) X. Yan, Z. Cao, A. Murphy, Y. Qiao, *J. Environ. Chem. Eng.* **2022**, *10*, 108130.

[11] a) K.-W. Lu, H.-L. Chen, H.-P. Chen, C.-C. Kuo, *Thin Solid Films* **2023**, *767*, 139672; b) Z. Song, H. Xiao, Y. Zhao, *Carbohydr. Polym.* **2014**, *111*, 442; c) C. Wang, P.-C. Lai, S. H. Syu, J. Leu, *Surf. Coat. Technol.* **2011**, *206*, 318.

[12] a) J. Belt, V. Utgikar, I. Bloom, *J. Power Sources* **2011**, *196*, 10213; b) M. Ecker, J. B. Gerschler, J. Vogel, S. Käbitz, F. Hust, P. Dechent, D. U. Sauer, *J. Power Sources* **2012**, *215*, 248; c) M. Ecker, N. Nieto, S. Käbitz, J. Schmalstieg, H. Blanke, A. Warnecke, D. U. Sauer, *J. Power Sources* **2014**, *248*, 839; d) S. Käbitz, J. B. Gerschler, M. Ecker, Y. Yurdagel, B. Emmermacher, D. André, T. Mitsch, D. U. Sauer, *J. Power Sources* **2013**, *239*, 572.

[13] D. G. Mackanic, M. Kao, Z. Bao, *Adv. Energy Mater.* **2020**, *10*, 2001424.

[14] a) Y. Dou, T. Pan, S. Xu, H. Yan, J. Han, M. Wei, D. G. Evans, X. Duan, *Angew. Chem., Int. Ed.* **2015**, *54*, 9673; b) L. Cui, J.-T. Yeh, K. Wang, F.-C. Tsai, Q. Fu, *J. Membr. Sci.* **2009**, *327*, 226.